Quarterly Progress Report

For Period

April 1 - June 30, 1965

FUNDAMENTAL STUDIES OF THE METALLURGICAL,
ELECTRICAL, AND OPTICAL PROPERTIES OF
GALLIUM PHOSPHIDE

Grant No. NsG-555

Prepared For

NATIONAL AERONAUTICS AND SPACE ADMINISTRATION
LEWIS RESEARCH CENTER
CLEVELAND, OHIO

Work Performed By

Solid-State Electronics Laboratories
Stanford University
Stanford, California

PROJECT 5108: A STUDY OF $GaAs_xP_{1-x}$

National Aeronautics and Space Administration
Grant NsG-555
Project Leader: G. L. Pearson
Staff: Yen-sun Chen

The object of this project is to evaluate the optical, electrical and
metallurgical properties of the $GaAs_xP_{1-x}$ alloy system. Among evaluations
of particular interest to us are the investigation of the crystal structure
and its imperfections by the Kossel line technique and by that of the lattice
absorption spectra as the mole fraction of GaAs, x, varies from 0 to 1.

Results reported last quarter[1] showed that two reflectivity maxima were
detected in the Reststrahlen band measurement. However, we were not able
to detect a distinct GaAs-like band in samples with x less than 0.70 and
therefore we were unable to establish the direction of the shift of this
band with respect to x. This was partially due to the instrumental diffi-
culty of resolving small signals from the noise and from the stray light
in the long wavelength end of the spectra. Attempts were made this quarter
to obtain a set of more reliable and better resolved reflectivity spectra
in the region of 20μ to 40μ. This was accomplished through the cooperation
of Professor W. G. Spitzer at the University of Southern California. Data
were taken on their single-beam instrument which is basically built around
a Perkin-Elmer Grating Monochromator operating in the region between 7μ
and 45μ; the instrument gave a resolution and an accuracy better than
$\pm 1/2$ cm^{-1}.

The data were taken point by point using a sample-in and sample-out method. The reflectivity spectra are shown in Fig. 1a, 1b, and 1c for samples with various values of x. Samples of 48 and 67.5 percent phosphorus were small in area and the discontinuity in the reflectivity spectra near 280 cm^{-1} was due to a change in gratings.

A.   DISCUSSION

1. The GaP-like band appears throughout the entire alloy system. As the mole fraction of phosphorus decreases, this band shifts toward longer wavelength (or smaller wave number) and decreases in strength.

2. The GaAs-like band appears only in alloys containing less than 48 percent P. If the band of the minority constituent is indeed due to the absorption of the vibration mode of that constituent in the host lattice of the majority constituent, then the experimental results agree with the theoretical prediction[2] that only a lighter mass impurity in a heavier host lattice gives certain localized modes appearing with frequencies above the range of the unperturbed modes.

3. Although there is a tendency for the minimum of the reflectivity spectra in the region of the GaAs-like band to shift toward longer wavelength as the mole fraction of arsenic decreases, there is very little shift in the Reststrahlen frequency.

4. The Reststrahlen frequency vs the composition of the alloy is plotted in Fig. 2. The frequencies are determined by picking the break point of the reflectivity maximum at the longer wavelength side[3] if the shape of the maximum is square-topped and by picking the frequency of the peak if the shape of the maximum is peaked. Also shown in Fig. 2 is the sum of those two bands which appear near 610 cm^{-1}. A band of such

frequency should appear in the absorption spectra and its strength should be comparable to that of a two-phonon absorption band. This is indeed so, as reported last quarter in that a new band in the two-phonon absorption spectra emerged at 610 cm^{-1} for compositions less than 48 percent P and its strength decreased as the mole fraction of P decreased.

B. THEORETICAL CONSIDERATIONS

In pure material a classical treatment of the Reststrahlen band gives fairly direct information about optically active phonons of zero wave vector.[4] A similar treatment is tried here for our alloy system. Three kinds of atoms are involved in the alloy; gallium atoms are located at one of the two face-centered cubic sublattices of the zinc-blende structure, while arsenic and phosphorus atoms are distributed randomly in the other face-centered cubic sublattice as far as the long wavelength classical approach is concerned. The equations of motion for these atoms can be described as follows:

$$m_a \ddot{u}_a = -\alpha (u_a - u_c) - x\eta (u_a - u_b) \tag{1}$$

$$m_b \ddot{u}_b = -\beta (u_b - u_c) - (1 - x) \eta (u_b - u_a) \tag{2}$$

$$m_c \ddot{u}_c = -x\beta (u_c - u_b) - (1 - x) \alpha (u_c - u_a) \tag{3}$$

where the subscripts a, b, and c represent P, As, and Ga atoms respectively, u_i's are the displacements, m_i's are the masses, x is the mole fraction of As, α and β are respectively the force constants between Ga and P and

- 3 -

between Ga and As as first nearest neighbors and η is the force constant between As and P as second nearest neighbors.

The assumptions made are the following:

1. The two sublattices vibrate against each other in the optical phonon mode as in pure material.

2. First nearest neighbor forces are considered; the only second nearest neighbor force considered is the force between As and P.

3. Let α, β, γ be represented by K, then

$$K = K_o (1 - \theta x) \tag{4}$$

where θ is determined by Grüneisen's Relation;[1] this corresponds to the change in the binding strength as the lattice constant is changed from that of GaP $(x = 0)$ to that of GaAs $(x = 1.0)$. θ is found to be 0.216 for pure GaP[1] and this value is used.

In the case of sinusoidal vibration, the frequency ω is determined by the following equation:

$$\begin{vmatrix} m_a\omega^2 - \alpha - x\eta & x\eta & \alpha \\ (1 - x)\,\eta & m_b\omega^2 - \beta - (1 - x)\,\eta & \beta \\ (1 - x)\,\alpha & x\beta & m_c\omega^2 - (1 - x)\,\alpha - x\beta \end{vmatrix} = 0 \tag{5}$$

This gives a trivial solution of $\omega^2 = 0$ for all values of x between 0 and 1.0, which is just the motion of the crystal as a rigid body. The following solutions are obtained for the extreme cases of $x = 0$ and $x = 1.0$:

for $x = 0$, $\qquad \omega^2 = \dfrac{\alpha_o}{m_a} \left(1 + \dfrac{m_a}{m_c}\right),$ $\qquad\qquad\qquad$ (6)

$\qquad\qquad$ or $\; = \dfrac{\beta_o + \eta_o}{m_b}$ $\qquad\qquad\qquad\qquad\qquad$ (7)

for $x = 1.0$, $\qquad \omega^2 = \left[\dfrac{\alpha_o + \eta_o}{m_a}\right] (1 - \theta)$ $\qquad\qquad\qquad$ (8)

$\qquad\qquad$ or $\; = \dfrac{\beta_o}{m_b} \left(1 + \dfrac{m_b}{m_c}\right) (1 - \theta)$ $\qquad\qquad\qquad$ (9)

Data points correspond to Eqs. 6, 8 and 9 are picked to determine α_o,

β_o, η_o, and the resulting values are

$$\alpha_o = 2.86 \times 10^6 \, gm \, cm^{-2}, \quad \beta_o = 3.32 \times 10^6 \, gm \, cm^{-2}, \quad \eta_o = 1.72 \times 10^6 \, gm \, cm^{-2}.$$

The dashed curves in Fig. 2 are the calculated results from Eq. 5 using

the above constants and, as can be seen, they give an exceedingly good fit.

The model proposed here, though based on simple first principles,

is physically sound, for it takes into account three important points

1) the As and P atoms are distributed "randomly" in the long wavelength

approach, 2) the effect of change in lattice constant on the binding force

between nuclei is considered, and 3) a force constant between As and P is

introduced as an interaction term in the alloy; this force constant at

extreme values of x is shared by twelve second nearest neighbors, thus

making it very small compared to the force constant involving nearest neigh-

bors. This model is thus favored over that discussed last quarter where only

the effect of change in lattice constant on the binding force between

nuclei was considered.

We wish to thank Professor W. Shockley for important contributions to the theoretical discussion given above.

REFERENCES

1. SEL Quarterly Research Review No. 12, Project 5108.

2. P. G. Dawber and R. J. Elliott, Proc. Roy. Soc. A 273, 222 (1963).

3. G. Picus, E. Burstein, B. Henvis and M. Hass, J. Phys. Chem. Solids, 8, 282, (1959).

4. M. Born and K. Huang, Dynamical Theory of Crystal Lattices. Oxford Press (1954).

FIGURE CAPTIONS

Fig. 1a, b, c   Reflectivity spectra of $GaAs_xP_{1-x}$ alloy samples in

Reststrahlen band region.

Fig. 2   Reststrahlen frequency vs composition.
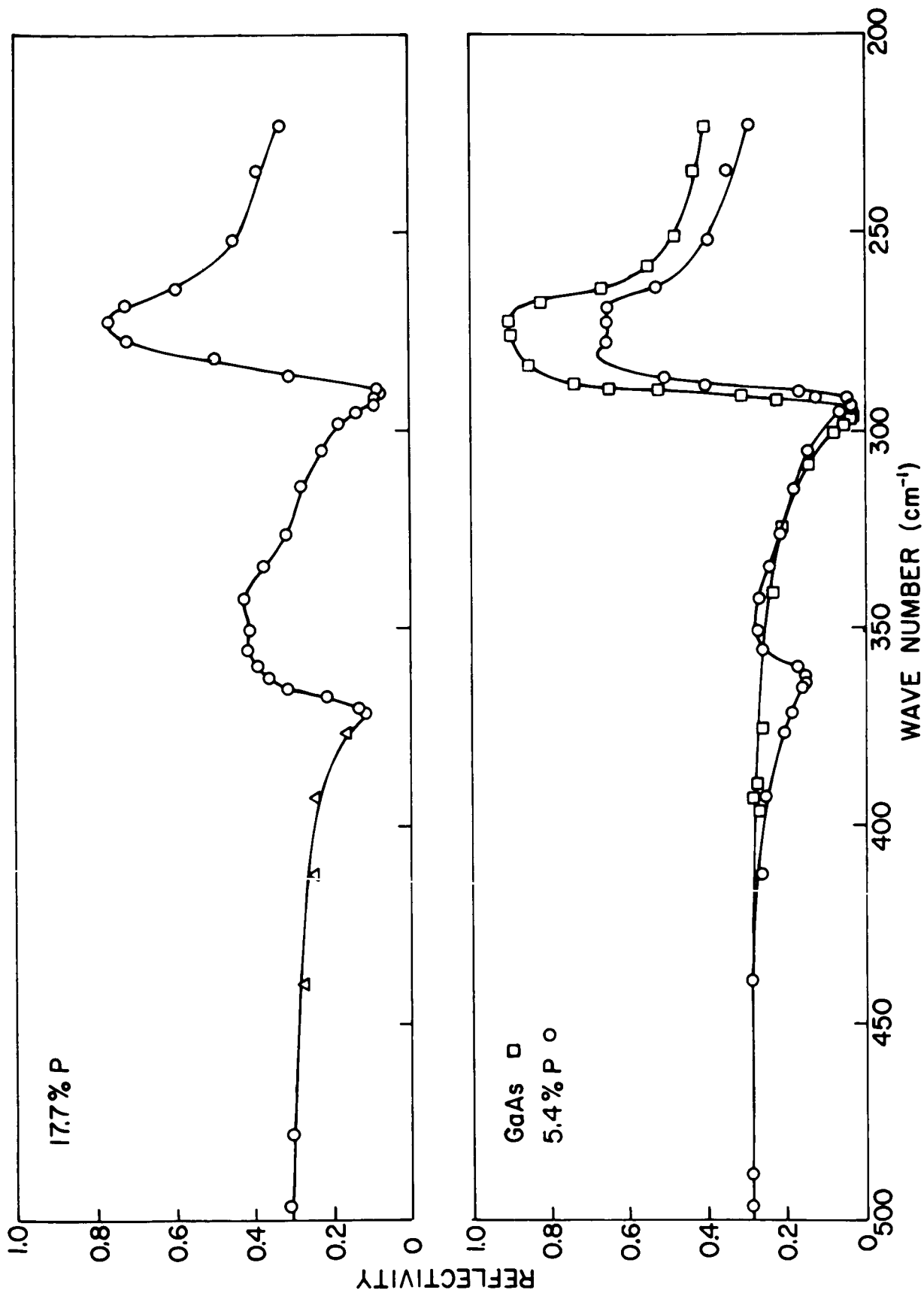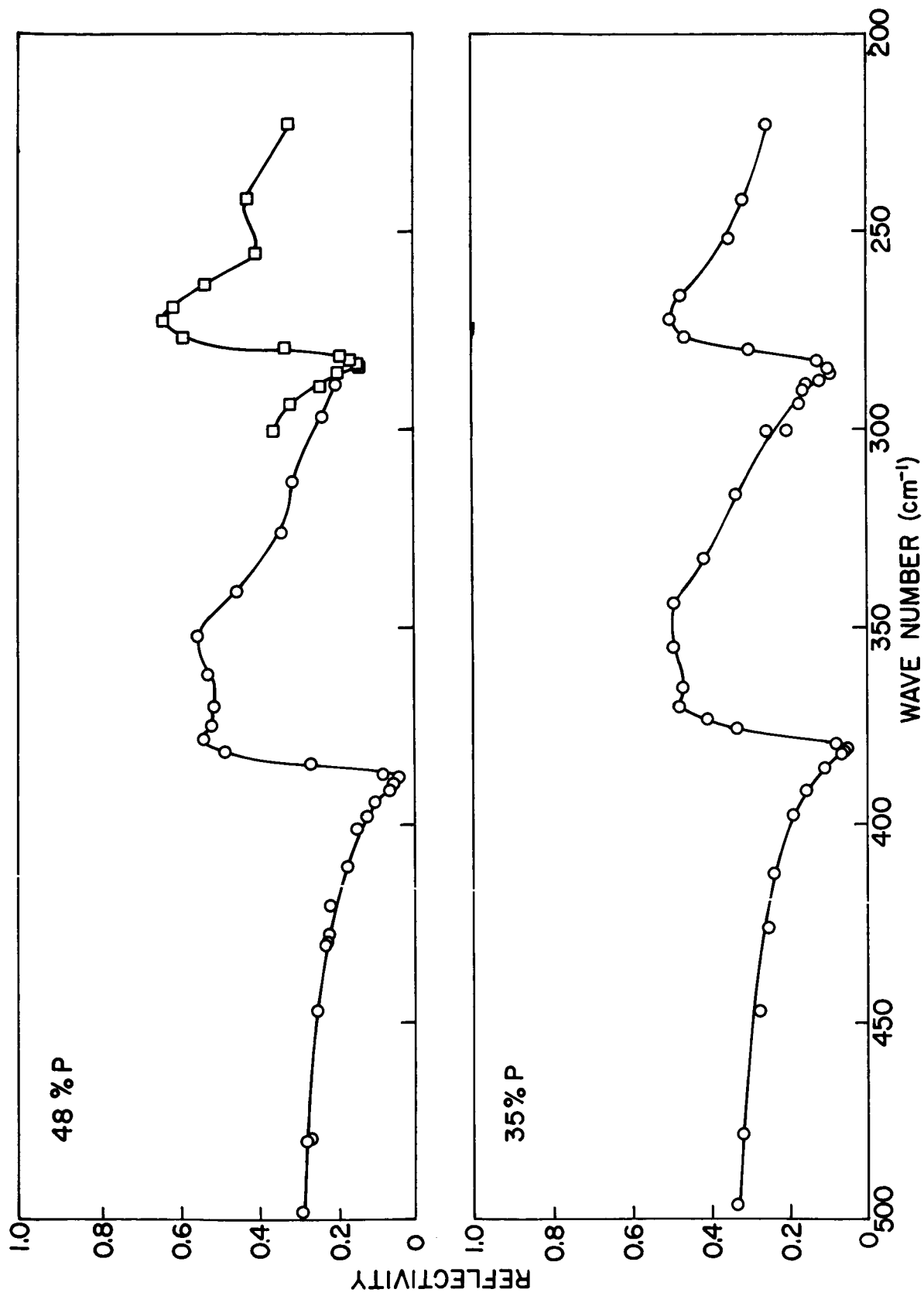
FIG. 1a.

17.7% P

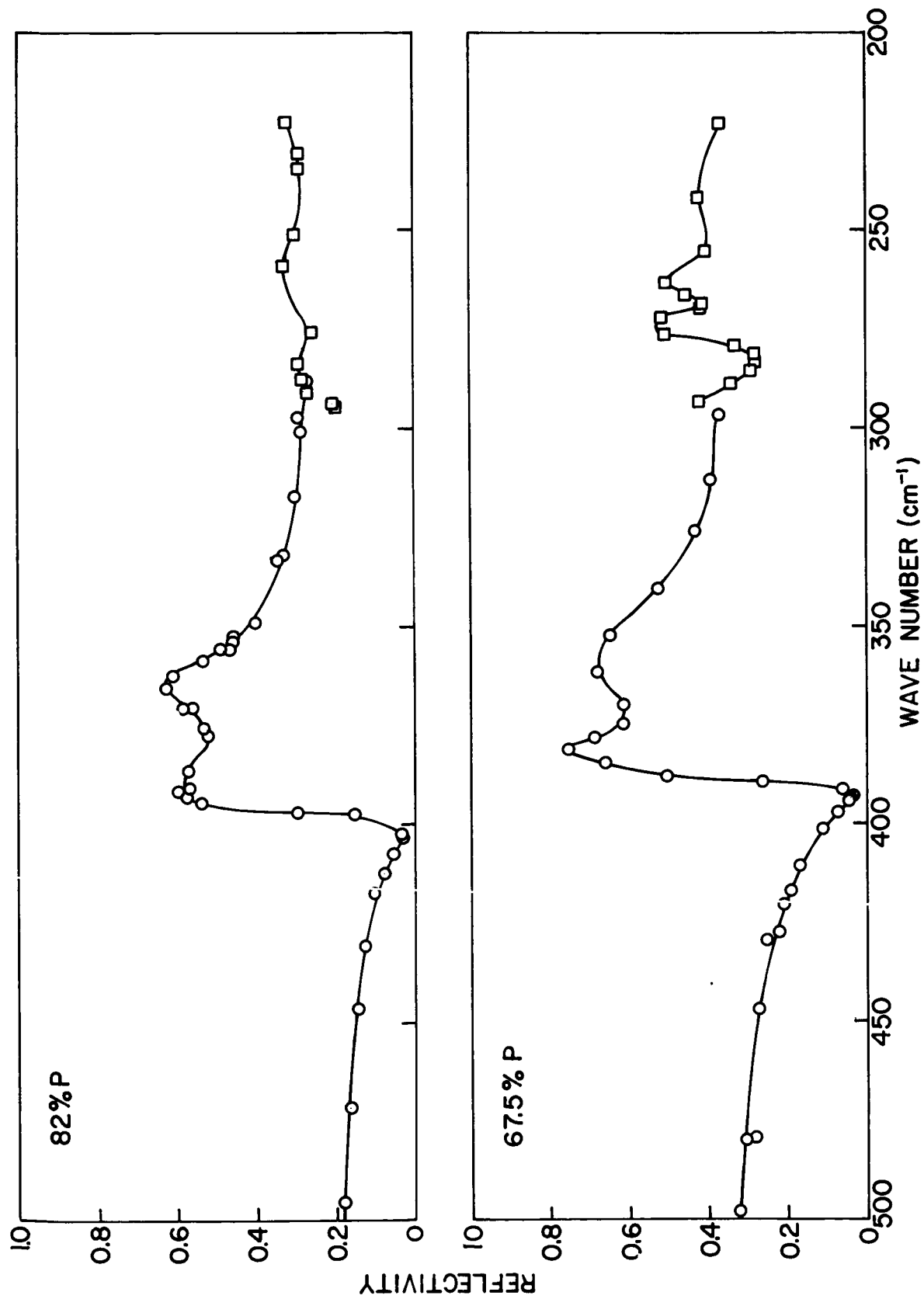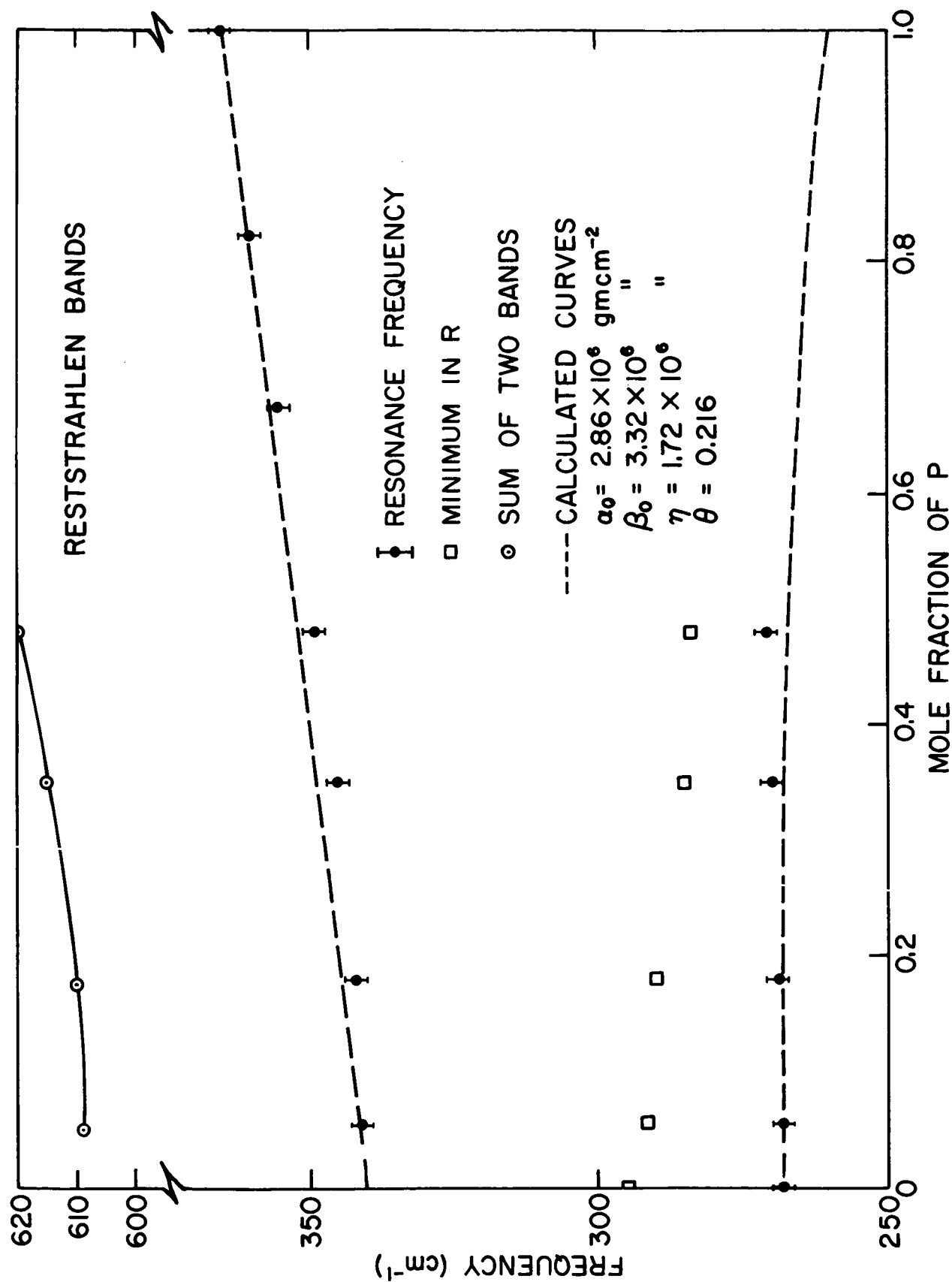GaAs □
5.4% P ○

REFLECTIVITY

WAVE NUMBER (cm⁻¹)

REFLECTIVITY

48 % P

35% P

WAVE NUMBER (cm⁻¹)

FIG. 1b.

FIG. 1c.

82%P

67.5% P

REFLECTIVITY

WAVE NUMBER (cm⁻¹)

RESTSTRAHLEN BANDS

⊦●⊣ RESONANCE FREQUENCY

□ MINIMUM IN R

⊙ SUM OF TWO BANDS

---- CALCULATED CURVES

$\alpha_0 = 2.86 \times 10^6$ gmcm^{-2}
$\beta_0 = 3.32 \times 10^6$ "
$\eta = 1.72 \times 10^6$ "
$\theta = 0.216$

FREQUENCY (cm^{-1})

MOLE FRACTION OF P

FIG. 2.

PROJECT 5109: EPITAXIAL GROWTH OF III-V SEMICONDUCTOR COMPOUNDS

The purpose of this project is to study the chemical, electrical

and optical properties of cobalt as an impurity in gallium phosphide.

The thermodynamic properties of ternary systems consisting of GaAs or

GaP and an added impurity are also under investigation.

A. INTRODUCTION

This study of cobalt impurities in GaP naturally divides itself into

three parts. Part one is the production of single crystals of GaP; work

on this part was reported in the last quarterly review. Part two is the

diffusion of radioactive Co into GaP in order to determine the diffusion

profile and solubility of Co in GaP; work on this part is reported below.

Part three, on which no experimental work has yet been done, is the measure-

ment of the optical and electrical properties of Co doped GaP.

During the quarter covered by this report a series of diffusions of

radioactive Co into gallium phosphide was done. The diffusion profile

and solubility of Co in GaP have been determined for a number of different

diffusion times and temperatures.

The method used to measure the solubility and diffusion profile are

discussed in section B below. The results of the diffusion and a dis-

cussion of the results are reported in sections C and D respectively.

B. EXPERIMENTAL METHOD

There are three parts to the Co radio-tracer diffusion experiment. The first part consists of evaporating radio-tracer Co onto the surface of the GaP crystal. Secondly, the crystal is sealed in an evacuated ampoule with a small quantity of phosphorus after which the crystal and ampoule are placed in a high temperature furnace. Finally, a disc is cut from the diffused crystal and the distribution of Co in the disc is determined by radioactive counting techniques. These three parts of the diffusion experiment are discussed in detail below.

In order to prevent the decomposition of the GaP the Co diffusions are done in sealed evacuated ampoules. Since the vapor pressure of Co is negligible at the diffusion temperatures it is not possible to simply seal a small piece of Co into the ampoule with the sample. It is necessary to either plate or evaporate a layer of Co onto the surface of the crystal before sealing the crystal into the ampoule. A layer of Co 55$\overset{\circ}{A}$ thick is needed to uniformly dope a 20 mil thick crystal with 10^{18} cobalt per cc. . Experiments showed that Co could neither be electro-lessly deposited nor easily electrially deposited onto GaP crystals. Further experiments showed that Co could be plated onto a tantalum wire evaporation filament which could then be used to put an evaporated layer of radio tracer Co onto the crystals. The major problem was obtaining electroplated layers which adhered to the evaporation filament.

The radio tracer Co was obtained from New England Nuclear Corporation as Co^{60} with a specific activity of 319 curies per gram dissolved in 2.24 ml of 1.4 N HCℓ solution. The solution contained a total of

2.96×10^{-7} moles of Co^{60}. In order to obtain a plating solution it was necessary to add non-radioactive Co to the solution and to reduce the pH of the solution. Nine normal KOH was chosen to reduce the acidity of the solution so that the acidity could be reduced without substantially increasing the volume of solution. The Co content of the solution was increased by adding enough $CoCl_2 \cdot 6H_2O$ so that the ratio of Co^{59} to Co^{60} was 495. Since the pH of an acid solution changes very quickly when a strong base is added, a number of trial solutions were made to determine exactly the amount of KOH needed to bring the solution to a pH near 7. The final solution was brought to a pH of about 7 with KOH and then buffered with boric acid at a pH of 5 ($60^{o}C$). The final composition of the plating solution is listed below:

Co^{60}	1.16×10^{-4}	molar
Co^{59}	5.73×10^{-2}	molar
K^{+}	1.14	molar
B_2O_3	0.294	molar
Total volume	1.14 ml.	Use at $60^{o}C$.

The experiment showed that solutions containing less Co did not plate well. In fact, the major limitation of this method of plating a wire and then evaporating onto a crystal is that the specific activity of the radio tracer must be reduced in order to obtain a workable plating solution. On the other hand, the method should be applicable to most of the radio tracers available in solution. The Co is plated onto tantalum because the electroplate would not adhere to tungsten.

The cathode efficiency of the plating solution has been determined. While Co can be in solution in either the form Co^{++} or the form Co^{+++}, the lower oxidation state, Co^{++}, is more common. Assuming that the Co in the solution is the form Co^{++}, the cathode reactions are:

$$Co^{++} + 2\ e^{-} \rightarrow Co \quad \text{and}$$
$$K^{+} + e^{-} \rightarrow K$$
$$2K + Co^{++} \rightarrow Co + 2K^{+}.$$
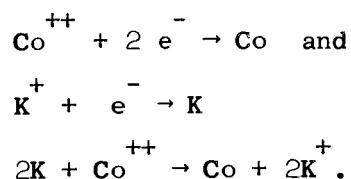
In either case two electrons are required to deposit one Co atom. This leads to an ideal plating rate of 18.3 micrograms of Co per milliamp-min. The results of plating four 0.010 tantalum wires at a current of 1 milliamp are shown in Fig. 1. The solid line corresponds to the ideal rate of 18.3 μg/min and the dash and the dotted line correspond to a rate of 16.5 μg/min. The latter rate corresponds to a cathode efficiency of 90% which seems quite good considering the very small amount of Co in the plating solution. It is possible that some Co oxide is plating out and that the weight of the deposit does not accurately measure the amount of Co transferred. However, since any oxide formed during plating is decomposed when the plating is evaporated from a filament, the deposition of some Co oxide does affect the ultimate utility of the plating. To summarize, Co can be plated onto tantalum filaments from a solution prepared from a commercially available solution of Co^{60} in HCℓ.

After the radio tracer Co has been plated onto the filament, the Co is evaporated onto a cleaned and polished GaP crystal. The crystals are

first lapped using 3200 grit abrasive and then polished using Linde A.
After polishing the crystals are cut, then soaked in warm KCN (10%
solution), and finally washed in deionized water and alcohol. The crystals
are then put into a small demountable vacuum chamber with the evaporation
filament. After the chamber is evacuated to about 10^{-6} torr the filament
is heated to a temperature of about $1900^{o}C$ and held at that temperature
for thirty seconds. Measurments of the radioactivity of the filament,
after it was fired, have shown that $1900^{o}C$ for thirty seconds is adequate
to evaporate all of the Co originally on the filament. After the evapo-
ration, the sample is ready to be sealed into a diffusion ampoule.

The diffusion is done by placing an ampoule containing the crystal
and a small quantity of phosphorus into a high temperature furnace. The
phosphorus is put into the ampoule to help prevent the decomposition of
the GaP and to fix the compositions of the chemical phases in the ampoule.
This last point is essential in the interpretation of the experimental
data. Using the Gibb's phase rule, if there are three phases in equi-
librium during the diffusion; a gas phase, a solid solution of Co in
GaP, and one of the cobalt phosphides, then there are two degrees of
freedom. One degree of freedom is removed when the temperature is
fixed at the diffusion temperature. Since there is still one degree
of freedome left, it is necessary to specify either the pressure or the
composition of one of the phases in order to completely specify the
system. However, because the ampoule represents a closed system, the
Duhem phase rule states that there is a total of two extrinsic and
intrinsic degrees of freedom. In a diffusion experiment in a sealed

ampoule these degrees of freedom are automatically removed when the
temperature, an intrinsic variable, and the volume, an extrinsic variable
are fixed. This means that one will always obtain the same solubility
of Co in GaP if in each experiment the same size crystal and the same
amount of Co are put into an ampoule of the same volume. However, if the
relation between sample size and volume is changed, perhaps in going from
a laboratory experiment to a large scale industrial process, then the
apparent solubility of Co will change. The easiest way to avoid this
dependence of the Co solubility on ampoule volume is to specify the
equilibrium conditions by a choice of two intrinsic variables. The most
convenient intrinsic variables are the temperature and the pressure. The
pressure is fixed by adding an amount of phosphorus, well in excess of
the amount which could react with the Co present, to the ampoule. Every
experiment to measure the solubility of Co will yield the same result if
the phosphorus pressure, assuming that phosphorus is the only constituent
of the gas phase, and the temperature are the same. Consequently, solu-
bility measurements are most useful if the temperature and the pressure
at which the solubility was established are given.

The ampoules used in the experiments to be described here were made
from 4 mm bore Englehard Suprasil or Thermal Syndicate Suprasil quartz.
A quartz plug was put into the ampoule to reduce the volume as much as
possible. After sealing, the free volume in a typical ampoule was about
0.1 cc. The phosphorus pressure inside a 0.1 cc ampoule containing
100μ grams of phosphorus, this is the amount used in our experiments,
is shown as a function of temperature in Fig. 2. The figure, which gives

the pressure due to the form P_4, the form P_2 and the total pressure, shows that the pressure in the ampoule is essentially constant over the temperature range 1000°K - 1500°K. The final steps in a diffusion are the heating of the sample in a high temperature furnace and finally quenching after the diffusion is complete. The sample is quenched so that the diffusion time can be easily and accurately determined.

After a crystal is removed from the diffusion ampoule it is rinsed in a dilute HNO_3 solution to remove any Co which might be on the surface. After the rinse one or more 0.10 inch discs are cut from the sample with an ultrasonic cutter. The disc is mounted in a precision lapping machine and thin layers, between one half and forty microns, are removed from it. The amount of material removed is determined by weighing the disc before and after lapping. The Co concentration in a layer lapped from the disc is determined from a measurement of the β activity of the alumina plate on which the disc was lapped.

The Co concentration is calculated from the activity of the disc in the following way. Let c be the number of counts per minute measured by the counter, minus the background, when a layer weighing $\Delta \omega$ grams has been lapped from the disc. An independent measurement using a Co^{60} standard shows that the ratio of counts to Co^{60} decays is 0.17. Then

$$[Co^{60}] = K \frac{c}{0.17 \Delta \omega} \rho_{GaP} \left(\frac{Co^{60}\text{'s}}{cc} \right), \qquad (1)$$

and the total Co concentration is given by

$$[Co] = K \cdot 495 \cdot \frac{c}{0.17 \Delta \omega} \rho_{GaP} \left(\frac{Co\text{'s}}{cc} \right). \qquad (2)$$

In the expressions above, ρ_{GaP} is the density of GaP (4.13 grams per cc), [Co] is the Co concentration measured in atoms per cc, and K is a constant related to the half life of Co^{60}. After inserting the value of K the expression is

$$[Co] = \frac{5.95 \times 10^{10} c}{\Delta\omega} \quad \frac{atoms}{cc} . \tag{3}$$

A straightforward calculation gives the thickness, t, of the layer removed as

$$t = 4.92 \, \Delta\omega \, (cm).$$

The Co diffusion profile is constructed by inserting the measured values of $\Delta\omega$ and c into the formulas given above. In Fig. 3 three typical Co diffusion profiles are shown.

C. RESULTS OF DIFFUSION EXPERIMENTS

The results of the diffusion experiments are best understood by referring to Figs. 3, 4, and 5. Fig. 3 shows the results of heating for 24 hours a Co evaporated GaP crystal which had a room temperature carrier concentration due to sulfur doping of 1.6×10^{18} carriers per cc. The figure shows that the profiles for the $1015^{\circ}C$ and $1117^{\circ}C$ diffusions consist of a narrow region near the front surface of the crystal in which the Co concentration decreases rapidly followed by a region of near-ly constant Co concentration. In the case of the $915^{\circ}C$ diffusion the Co concentration falls rapidly near the surface and then continues to vary

for another 100 microns before the profile becomes flat. The initial
sharp fall in the profiles is probably a manifestation of the presence
of a phosphide of cobalt on the surface of the diffused disc. Because
the disc is not lapped absolutely parallel to the Co evaporated face,
the presence of a layer of high Co concentration on the surface gives
rise to a region of apparently rapidly decreasing concentration. The
1015°C and 1107°C profiles suggest that the Co concentration has reached
the limit set by the solubility of cobalt. More data is needed to
properly interpret the 915°C profile.

In Fig. 4, the results of 1015°C diffusions for 7, 24, and 49 hours
are plotted on the same graph. All of the crystals were cut from the
same epitaxial slice as the crystals mentioned in reference to Fig. 3.
The figure shows that the profile has reached its final shape after seven
hours of diffusion. This data supports the conclusion that the profiles
in Fig. 3 represent the solubility of Co in GaP. The figure also shows
the spread in the data from which the profiles were constructed. The
line has been drawn through the 24-hour data because there was the least
spread in those experimental points. Diffusion profiles resembling those
shown in Figs. 3 and 4 have also been measured in lightly sulfur doped
material.

The results of the diffusions into the heavily sulfur doped GaP
(1.7×10^{18} carriers/cc) are shown again in Fig. 5. In this figure
the Co concentration 100 microns below the surface is plotted as a
function of the reciprocal diffusion temperature. The Co concentration
100 microns below the surface of lightly sulfur doped (7×10^{16} carriers/cc)
samples is also plotted in this figure. It is seen that all of the data

from the heavily doped sample and the 1200°C data from the lightly doped sample lie on a single straight line. However, the 1117°C and 1160°C data for the lightly doped sample lie well below the line.

D. DISCUSSION

Thermodynamics can be applied to the analysis of the results of a diffusion which has continued long enough for equilibrium to be established among the phases in the ampoule. The flat diffusion profiles shown in Figs. 3 and 4 suggest that equilibrium was established during the diffusion. Particularly, the profiles suggest an equilibrium between a phosphide of Co, let us say CoP_x, a GaP-Co solid solution and a gas phase. Since a straight line can be drawn through a number of the solubilities in Fig. 5 there is a tendency to argue that

$$[Co] = [Co^o] \exp\left(-\frac{b}{kT}\right) \tag{4}$$

and to identify b with an enthalpy of solution. Here $[Co]$ is the Co concentration, T is the absolute temperature and k is Boltzmann's constant. If the Co lies solely on interstitial sites so that the solid solution accurately consists of a solute, Co, dissolved in a solvent, GaP, then simple thermodynamical arguments show that for small cobalt concentrations the concentration should obey Eq. (4). If, on the other hand, any of the Co is on substitutional sites, then there is no simple physical interpretation of the constant b. Since we expect that some of the Co is on substitutional sites, we do not interpret b as an enthalpy of solution. The flat diffusion profiles suggest that the cobalt may be

- 10 -

rapidly diffusing interstitially and then moving onto substitutional

sites. At this time the only evidence to support this view is the

rapid diffusion through the crystal.

The error in the measured concentration must be calculated if the

data is to be meaningful. As was mentioned earlier, the formulation of a

working Co plating solution required the addition of Co^{59} until the ratio

of Co^{60} to Co^{59} was 495. As a result most of the Co in the sample after

a diffusion is not radioactive and hence does not affect the β counter.

This means that the activity of a thin layer lapped from a diffused disc

is very low and that the counting error is quite large. For example, in

a particular lap 75μ grams, which is average for our experiment, are

removed and then counted to yield 60 counts per minute. The background

is 20 $\pm$ 3 counts per minute. Hence the corrected counting rate is

60 - (20 $\pm$ 3) or 40 $\pm$ 3. Taking one standard deviation at 40 gives

40 $\pm$ 9 counts as the probable range for the number of counts; i.e.,

a probable error of around $\pm$ 22%.

From Eq. (3) we obtain

$$[Co] = 3.2 \times 10^{16} \pm 22\%, \tag{5}$$

for c = 40 $\pm$ 9 counts per minute.

Similar calculations show that the probable error for a number of

values of $[Co]$ is about:

[Co]	error
8×10^{15}	$\pm 60\%$
3×10^{16}	$\pm 25\%$
3×10^{17}	$\pm 8\%$

A conservative estimate of 3% for the error in $\Delta\omega$ and in the quantities used to determine the constant 5.95×10^{10} has been included in the errors listed above. Because the probable error in any one measurement of the concentration is quite large, no attempt has been made to fit a curve through every measured point. Instead the diffusion profiles have been constructed by drawing a smooth curve through the center of the distribution of the data points. The spread in the data and the result of fitting a single smooth curve to the data are shown in Figs. 3 and 4.

E. CONCLUSION

Radiotracer Co has been plated from solution onto evaporation filaments from which it has been evaporated onto polished pieces of GaP. The cobalt has been diffused into the GaP at high temperatures and the diffusion profile has been determined using radioactive counting techniques. The results of the diffusion experiments are presented in Figs. 3 and 4 of this report.

FIGURE CAPTIONS

Fig. 1   Rate of plotting Co from the radiotracer plating solution.

Fig. 2   The total pressure and the contributions to the pressure from

P_2 and P_4 inside a 0.1 cc ampoule containing 100 μg of phosphorus.

Fig. 3   The results of 24 hours diffusions at $915^{\circ}C$, $1015^{\circ}C$, and $1117^{\circ}C$.

Fig. 4   The results of 7, 24, and 50 hours diffusions at $1015^{\circ}C$.

Fig. 5   The cobalt concentration 100μ below the diffused surface as

a function of temperature and initial doping.
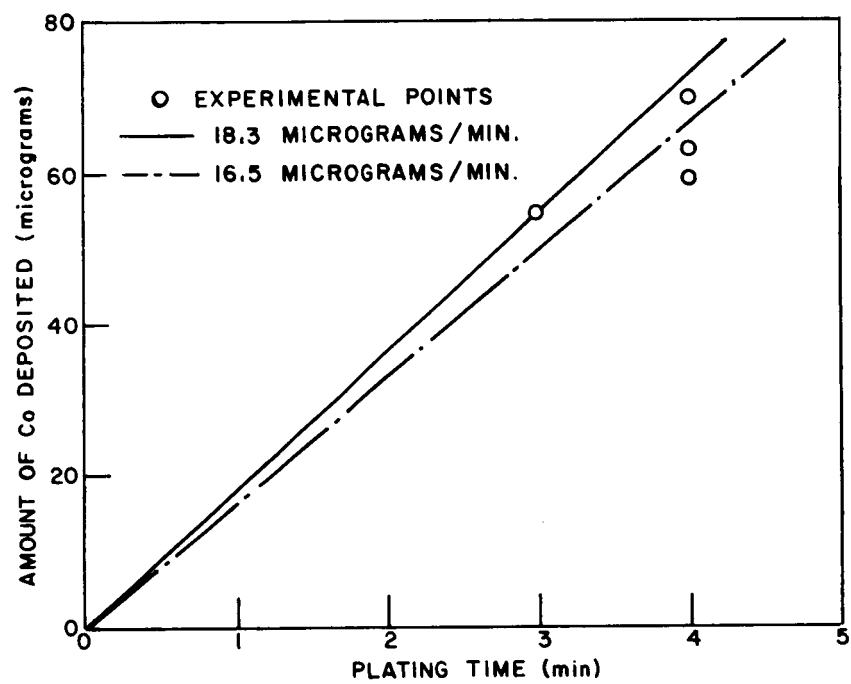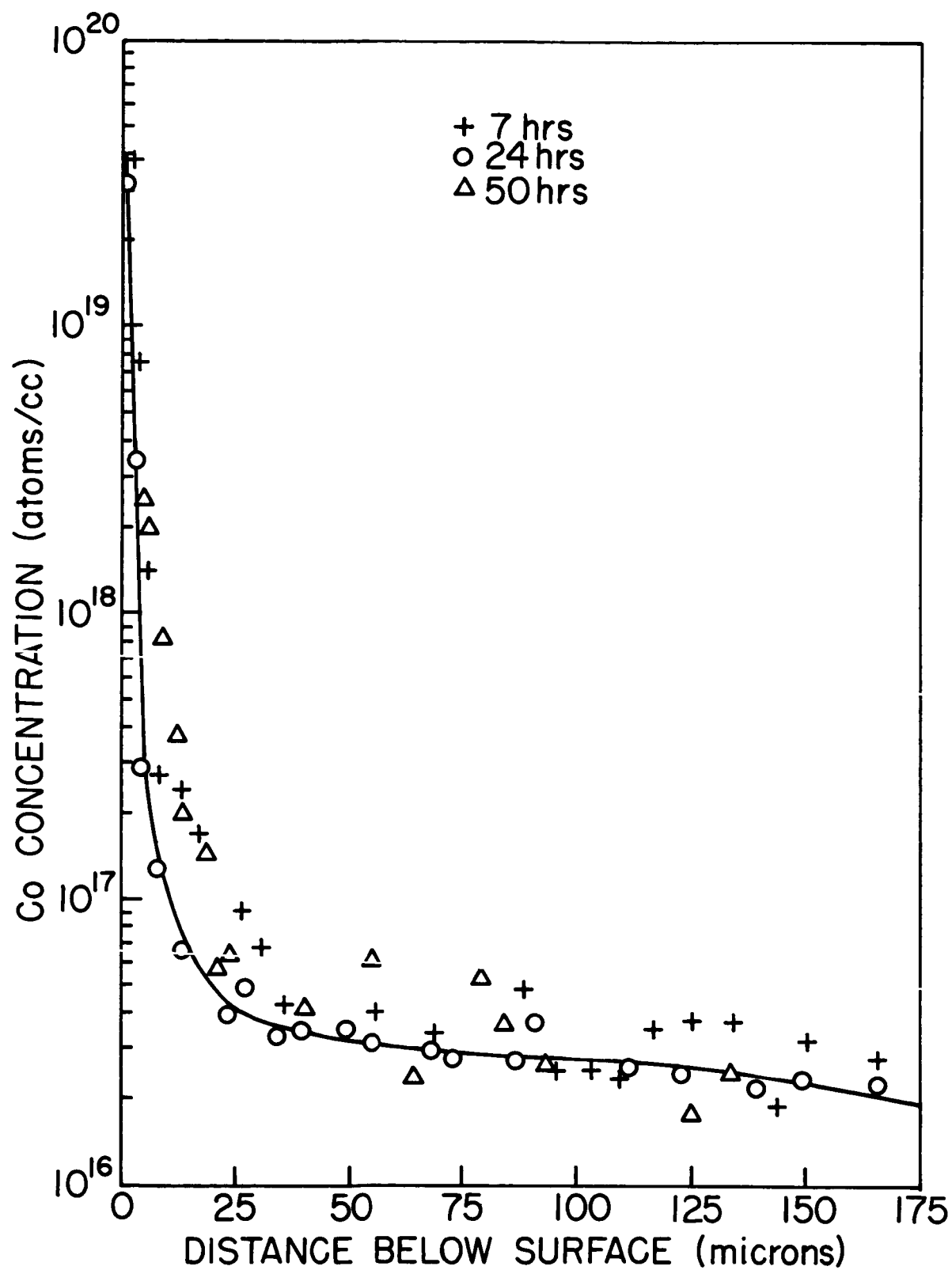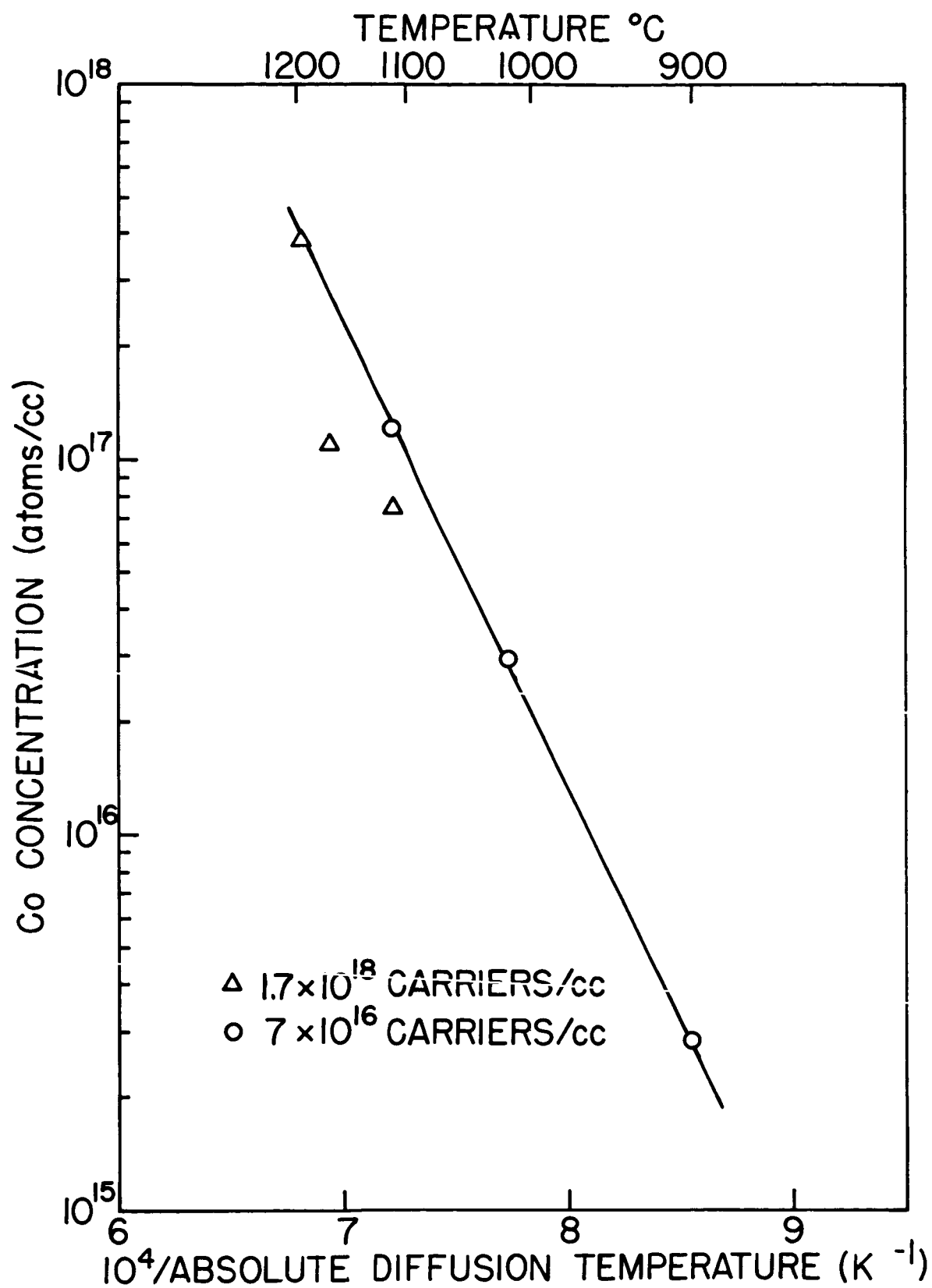
FIG. 1.
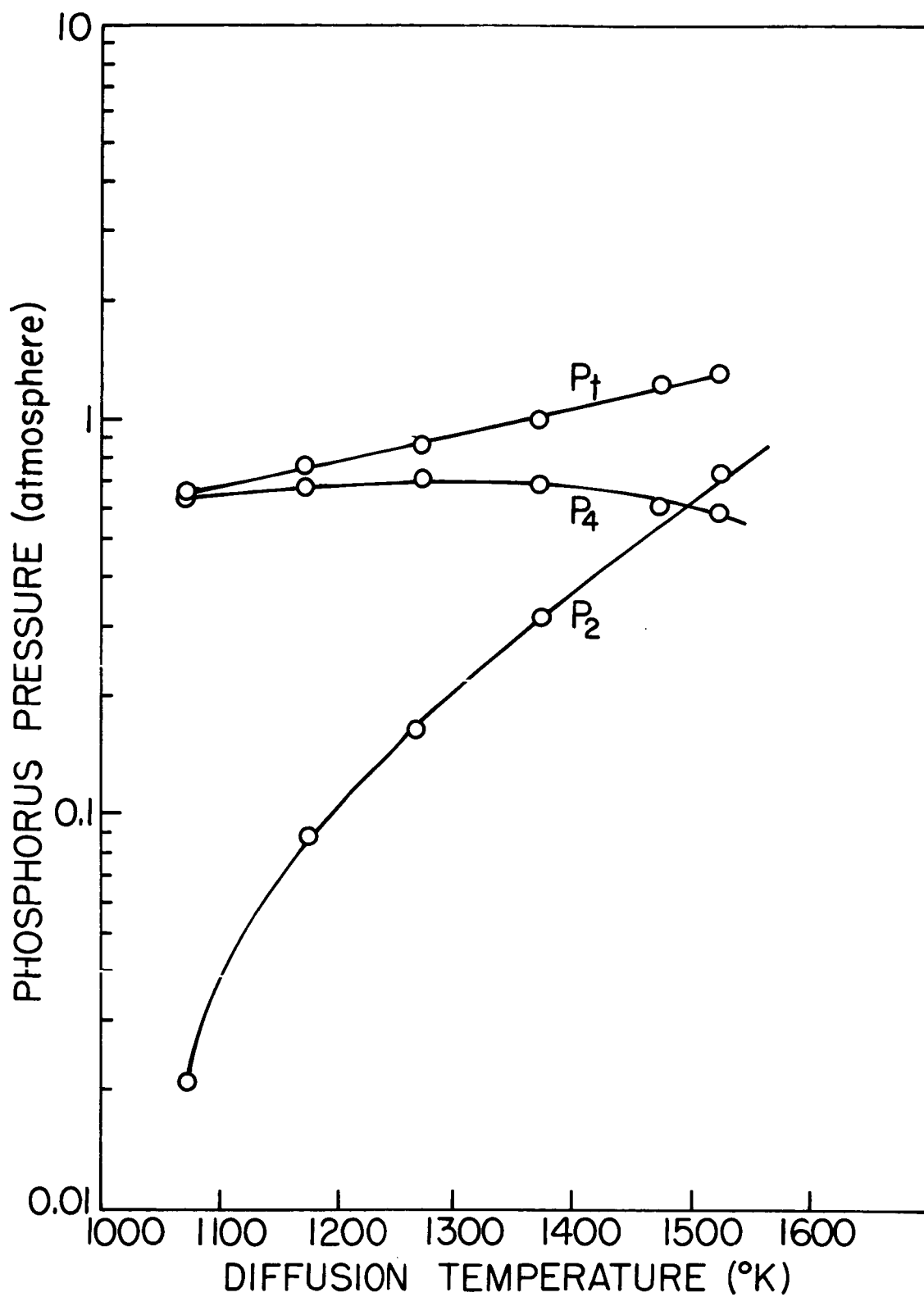
FIG. 2.
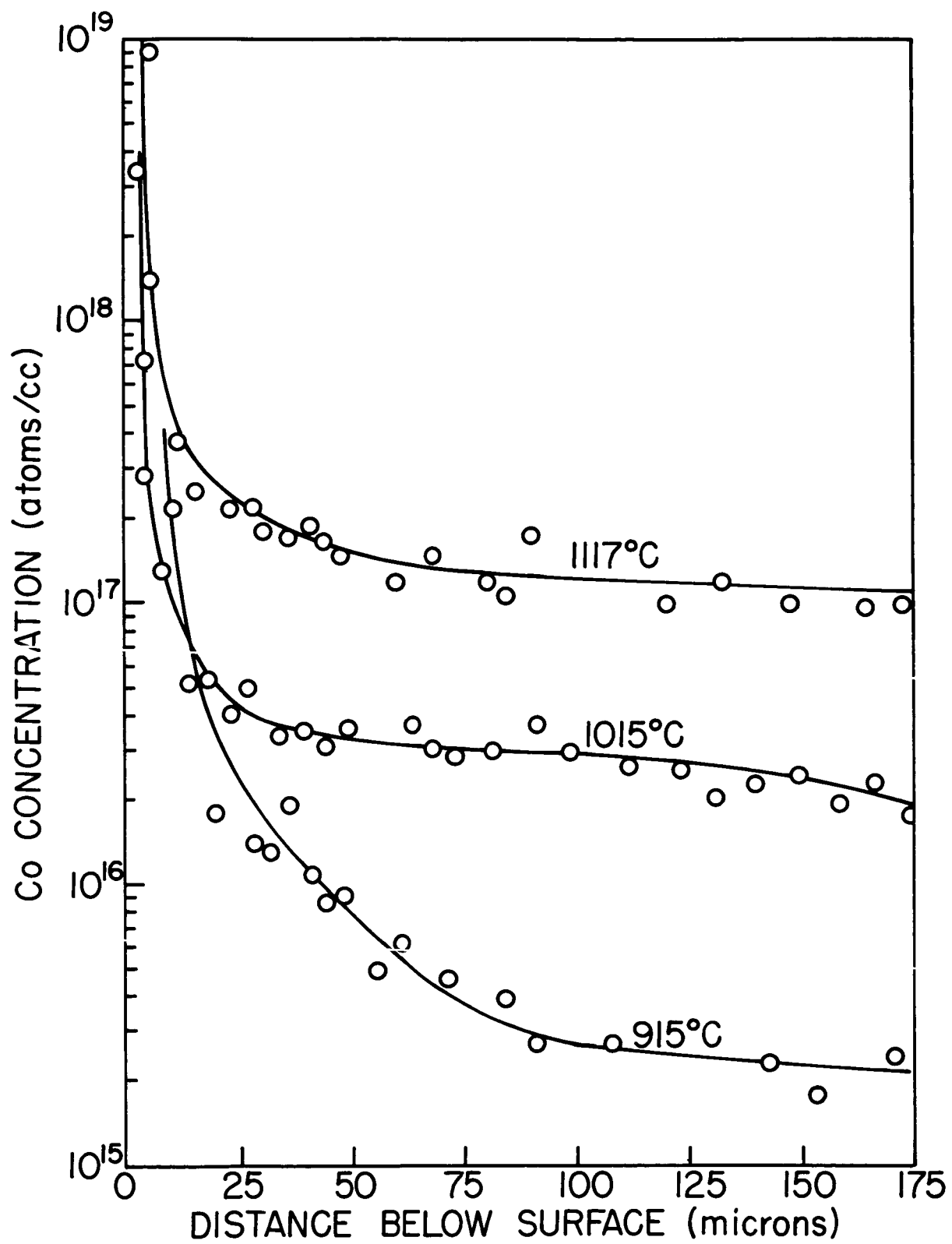
FIG. 3.

FIG. 4.

FIG. 5.

PROJECT 5112: THE PROPERTIES OF RECTIFYING JUNCTIONS IN $GaAs_x P_{(1-x)}$

National Aeronautics and Space Administration
Grant NsG-555
Project Leader: G. L. Pearson, J. L. Moll
Staff: T. Koike

The purpose of this project is to study the properties of rectifying

junctions in GaP and $GaAs_x P_{(1-x)}$. It is planned to investigate both

metal barriers and p-n junctions. During the past quarter a sulfur-doped

n-type single crystal of GaP was grown by the epitaxial method and alloyed

p-n junction diodes were prepared. The electrical properties of these

diodes were studied over a wide range of temperatures and the results are

reported below.

I. CRYSTAL GROWTH

A sulfur-doped n-type GaP single crystal was grown by the open-tube

method developed at this laboratory.[1] The hydrogen gas stream was passed

over sulfur which was maintained at a constant temperature with a bath

of boiling acetone (b.p. = 65°C). The vapor pressure of sulfur at this

temperature is about 4.4×10^{-4} mm Hg.[1] This value of vapor pressure

was chosen to produce a donor density in the range of 10^{16} cm^{-3}. A single

crystal 0.040 in thick was obtained by this method.

II. RESISTIVITY MEASURMENTS

After the crystal was grown, a small rectangular sample was cut in

order to make resistivity measurements. The sample was polished, lapped,

and then etched in aqua regia for about 1 min. before alloying the ohmic

contacts. Several tin dots were alloyed in a Marshall furnace for 10

minutes at 500°C with a hydrogen flow rate of 1 cu.ft./hr. The sample

dimensions are shown in Fig. 1.

This sample was then tested on the diode curve tracer to investigate

the properties of the ohmic contacts; no rectification was observed. The

donor density N_D can be calculated from the equation

$$N_D = \frac{1}{q\,\mu_n\,\rho} \tag{1}$$

Since the sample is photosensitive, the resistivity measurements were

performed in the dark. The resistivity of the crystal measured 2.1Ω cm.

Using Eq. (1) and $\mu_n = 100$ cm^2/volt-sec, we obtain a donor density of

3×10^{16}/cm^3 as expected from the growth parameters.

III. PROPERTIES OF ALLOYED pn JUNCTIONS

Several alloyed pn junctions were made from the grown crystal by the

following procedure: 1) The crystal was cut into small samples of about

20 mils in thickness, 2) These small samples were lapped and polished

with #1200 abrassive, and 3) The samples were then etched in aqua regia

for about 1 min, immediately prior to the alloying process.

The alloying process consists of two steps. A tin pellet was first

placed on one side of the sample and alloyed in the Marshall furnace

for 5 minutes at 500°C with a hydrogen flow rate of 1 cu.ft./hr. Then

the sample was quickly etched in aqua regia for 10 seconds to remove

the surface contamination. This was followed by the alloying of a tin

(99%) - zinc (1%) dot on the other side for 5 - 10 minutes under the

same alloying condition. This alloying process actually includes the diffusion of zinc into the n-type GaP to make the pn junction. The sample was again etched in aqua regia for 10 - 20 seconds after the alloying process.

A. GENERAL V-I CURVES

Several diodes were first tested by the diode curve tracer in order to check their general characteristics. We found some evidence that the reverse breakdown voltage was related to the alloying time. The result of such evidence is shown in Fig. 2. The data were taken on two different diodes, fabricated from the same crystal. The alloying times of the pn junctions were 10 minutes for Diode A and 5 minutes for Diode B, respectively. Diode A showed a breakdown voltage of about 10 volts. A similar result has been reported by Gershenzon and Mikulyak.[2]

B. CAPACITANCE VS VOLTAGE

The relation between the junction capacitance and the applied voltage was measured on Diode B. The result is plotted in Fig. 3. This result indicates that the diode has an abrupt junction. Gershenzon and Mikulyak[2] and Allen, et al[3] have reported the observation of an anomalous increase in capacitance at reverse voltages of about 3 volts in some diodes. This behavior was not observed in Diode B.

C. TEMPERATURE DEPENDENCE OF JUNCTION CHARACTERISTICS

The V-I curves were obtained by the diode curve tracer at three different temperatures (300°K, 396°K, and 504°K). Diode B was mounted inside a specially prepared copper block and heated on a hotplate.

The temperature was measured with a platinum-platinum 13 percent rhodium thermocouple which was also inserted in the copper block. The diode performed perfectly well up to 504° K (maximum temperature of the hot-plate) and no damage was found after the experiment. It should also be noted that this heat treatment actually improved the quality of the diode. The diode V-I curve was again observed on the oscilloscope at room temperature after the heating cycle. Increases in the forward current and the reverse breakdown voltage were observed. These results are shown in Fig. 4.

D. DETAILED FORWARD CHARACTERISTICS

Diode B was measured carefully up to 4 volts and a semilog plot of the data is shown in Fig. 5. In the low bias voltage range the result consists of two distinct straight lines. Between 0.25 and 0.6 volts, the current is given by

$$I \sim \exp\left(\frac{qV}{6.92kT}\right).\tag{2}$$

This is an anomalous dependence which cannot be explained by the recombination current.[4] Between 0.6 and 0.72 volts the current is in the form

$$I \sim \exp\left(\frac{qV}{2.33kT}\right).\tag{3}$$

At about 0.75 volts, the curve changes to another slope given by

$$I \sim \exp \left(\frac{qV}{1.22kT}\right). \tag{4}$$

This curve, however, is soon affected by the series resistance. A value of $10^4\Omega$ is obtained from the plot between 1.0 and 1.4 volts. This value decreases as the applied voltage is increased. From the data between 2.0 and 4.0 volts we obtained 70Ω for the series resistance. This resistance is actually an order of magnitude higher than the bulk resistance of the junction. We noticed in the resistivity measurement that there was no anomalous resistance between the bulk and the ohmic contacts. This may indicated that the anomalous resistance exists near the injection region. A similar result was observed by Allen, et al..[3] They postulated an impurity of sufficient concentration in the junction region that it could prevent the quasi-Fermi level from rising.

IV. REMARKS

We have measured some electrical properties of pn junctions fabricated from the same single crystal. The results indicate that the tin ohmic contact to low resistivity n-type GaP is of good quality. The temperature measurement shows promise for even higher temperature operation if a suitable alloying material is found. The capacitance measurement showed that the junction was abrupt. If we compare the breakdown voltage with those of silicon and germanium, the result falls in between silicon and germanium for $N_D = 3 \times 10^{16}/cm^3$.[5]

The anomalous behavior of the V-I curve below 0.7 volts implies some other contribution in addition to the recombination current described

by Sah, Noyce, and Shockley.[4]   One possibility may be surface currents and another possibility may be forward tunnelling current through some impurity level with a sufficient concentration.   This postulate also seems to be consistent with the existance of the extra high series resistance.   Further investigation will be necessary to understand these anomalies.

REFERENCES

1.   Y. S. Chen, SEL Quarterly Research Review No. 10 and 11; D. H. Loescher, SEL Quarterly Research Review No. 12.

2.   M. Gershenzon and R. M. Mikulyak, J. Appl. Phys. $\underline{32}$, 1338 (1961).

3.   J. W. Allen, M. E. Moncaster and J. Starkiewicz, Solid-State Elec., $\underline{6}$, 95 (1963).

4.   C. T. Sah, R. N. Noyce and W. Shockley, IRE $\underline{45}$, 1228 (1957).

5.   J. L. Moll, Physics of Semiconductors, p. 234, McGraw-Hill, (1964).

FIGURE CAPTIONS

Fig. 1   Sample dimension for resistivity measurements.

Fig. 2   V-I curves:

        a)   Diode A   (Alloyed for 10 minutes).

        b)   Diode B   (Alloyed for 5 minutes).

Fig. 3   Capacitance vs applied voltage for Diode B.   The area is
4.3×10^{-3} cm^2.

Fig. 4   Temperature dependence of V-I curves on Diode B.

        a)
          1.   300°K

          2.   396°K

          3.   504°K

        b)   Room temperature V-I curve after heating.

Fig. 5   Forward V-I characteristics of Diode B.

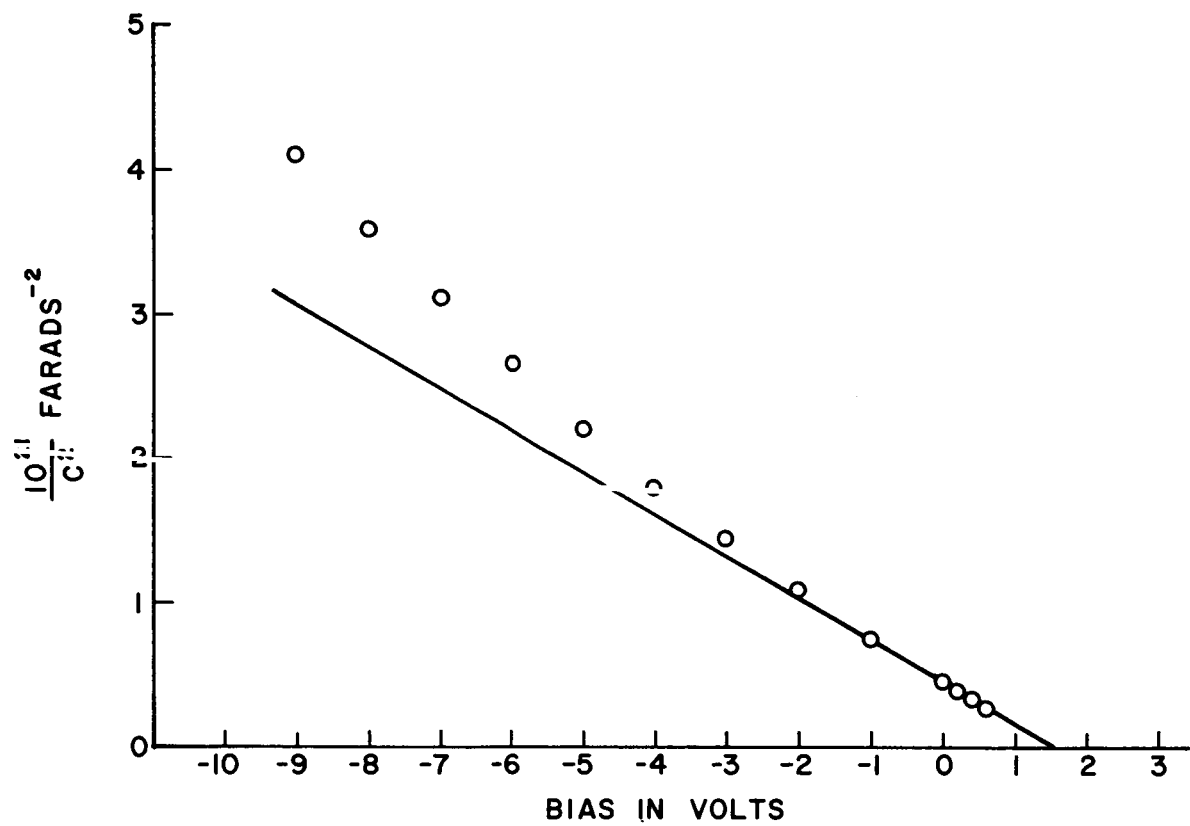TIN CONTACTS

1.06
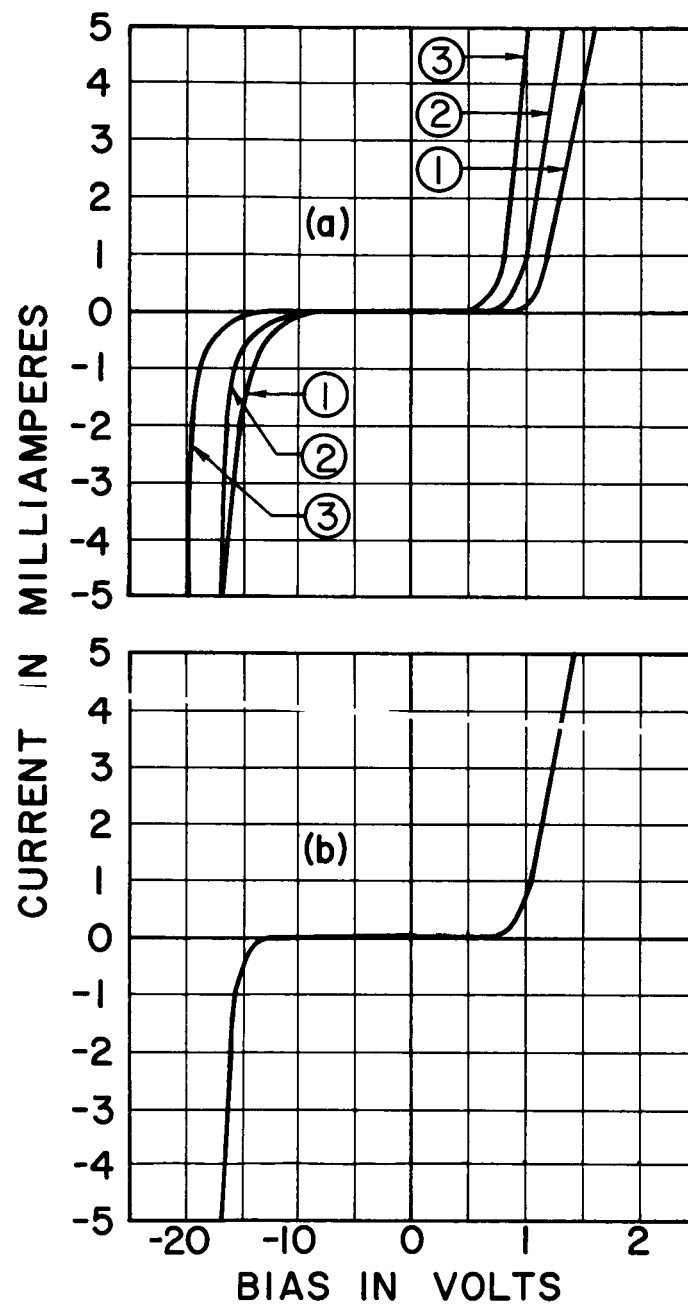
0.573

2.35

3.90

UNITS IN MM
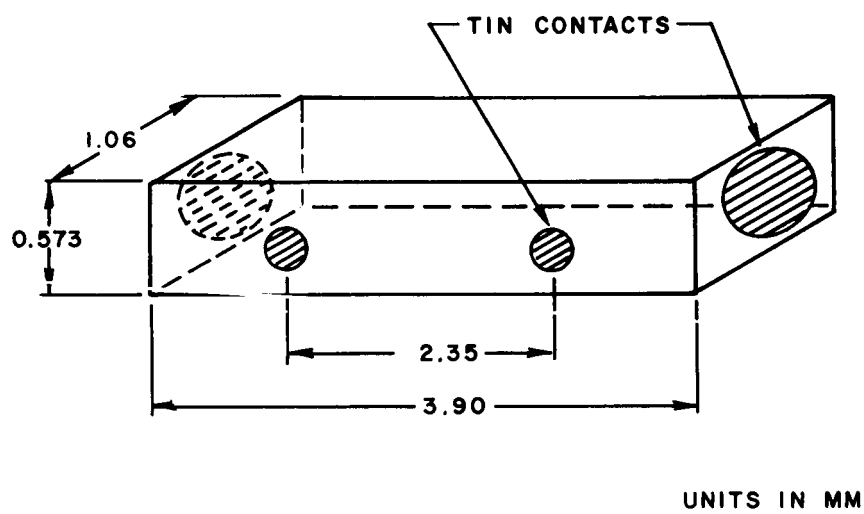
FIG. 1.
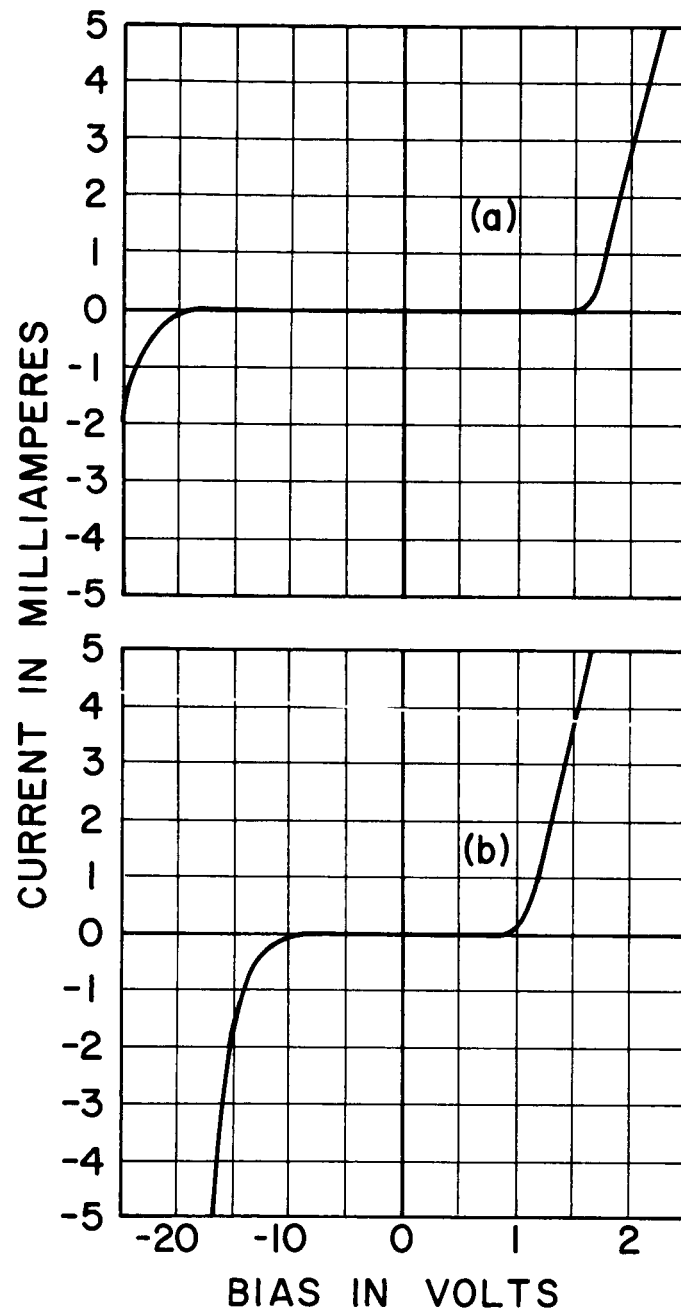
FIG. 2.

FIG. 3.

FIG. 4.
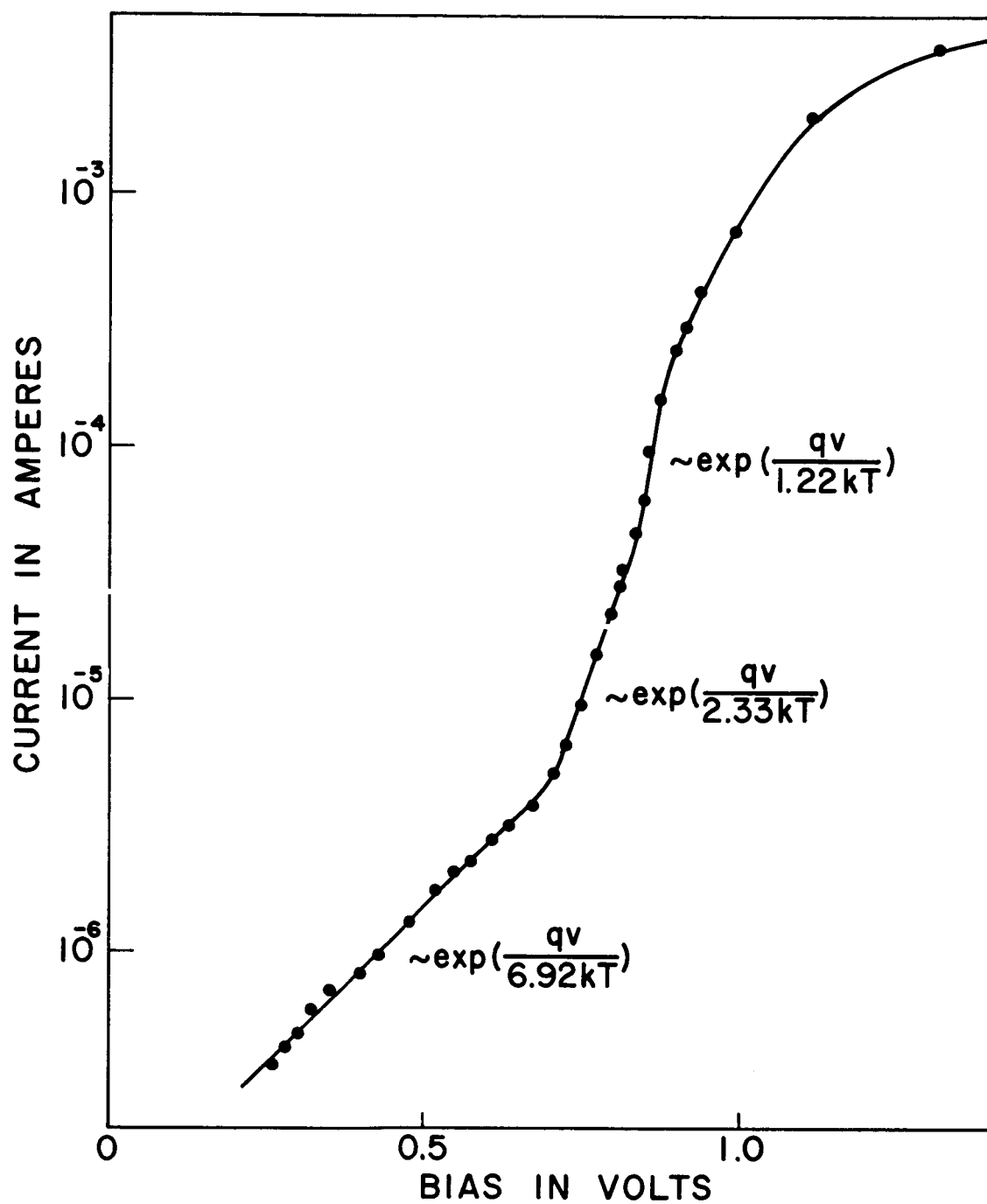
FIG. 5.

PROJECT 5114:   SEMICONDUCTING PROPERTIES OF GALLIUM PHOSPHIDE

The purpose of this project is to study the properties of GaP and $GaAs_xP_{1-x}$ relevant to their use as semiconducting materials.

In order to account for the concentration dependence of the diffusion of zinc into GaP and GaAs, Chang and Pearson[1] used a model in which zinc occurs either substitutionally or interstitially. The substitutional zinc atoms can be neutral or ionized, i.e. the holes can be localized at the zinc sites. On the other hand low temperature measurements of Hall effect[2] show that an impurity band is formed at concentrations as low as 2.10^{17} cm^{-3}, indicating that the holes are not localized on individual zinc atoms. The objection is sometimes raised that the interpretation of the diffusion data is inconsistent with the electrical measurements.

The resolution of the contradiction may be found by adapting Joffe's ideas concerning the existence of non-localized band states. If the mean free paths for lattice scattering is less than the mean distance between zinc atoms, then there will be no phase coherence between adjacent impurities and the holes can be localized. This condition holds at high temperatures, as in diffusion. If the mean free path for lattice scattering is much greater than the distance between zinc atoms, then non-localized bands can form at high enough zinc concentrations. This condition holds at low temperatures.

It is difficult to make these criteria quantitative, since there are no measurements reported on the mobility of holes in GaAs or GaP at high temperatures. By extrapolating data obtained below room temperature,[2] we find that for an impurity concentration of 10^{19} cm^{-3} the lattice mean free path equals the mean impurity spacing at about 600°K in GaAs. It appears that at all diffusion temperatures used in the preparation of pn junctions the assumption of Chang and Pearson of the existence of ionized and neutral zinc is justified. At low temperatures, for instance in room temperature precipitation, other conditions may apply.

1. L. L. Chang, G. L. Pearson, J. Appl. Phys. 35, 1960 (1964).

2. D. Meyerhoffer, Proc. Int. Conf. Semiconductors, Prague, 1960, p. 958.